Conformational Change Induced Reversible Assembly/Disassembly of Poly-L-lysine-Functionalized Gold Nanoparticles

Yi Guo,[†] Yudan Ma,[†] Li Xu,[‡] Jun Li,[†] and Wensheng Yang*[,†,‡]

Key Laboratory of Surface and Interface Chemistry of Jilin Province, College of Chemistry, Jilin University, Changchun, 130012, People's Republic of China, and Key Laboratory for Molecular Enzymolozy and Engineering of Ministry of Education, Jilin University, Changchun, 130021, People's Republic of China

Received: March 12, 2007; In Final Form: May 6, 2007

The poly-L-lysine-functionalized gold nanoparticle (PLL-GNP) was found to undergo reversible assembly/disassembly in the range of pH from 6.5 to 11.0 at room temperature. At a high pH value, the deprotonated lysine residues allow the formation of α-helix and β-sheet structures at the expense of a part of random coil and β-turn structures, thus inducing the assembly of GNPs. With a decrease of pH to 6.5, the assembly of GNPs is disrupted due to the conversion of the α-helix and β-sheet back into the random and β-turn. It is identified that the formation/collapse of an antiparallel β-sheet structure among PLL chains from adjacent GNPs is responsible for reversible pH-dependent assembly/disassembly of GNPs. Since the conformation-induced assembly/disassembly process of the PLL-GNP can be well recognized by a shift of the surface plasmon resonance band of the GNP and the color change of the solution, this study presents the possibility of following the conformation change of a peptide by monitoring the spectral change of the GNP.

Introduction

Biomolecules with intrinsic character of reversibility, such as DNA, proteins, and peptides, provide us the opportunity to assemble inorganic nanoparticles into nanostructures which can undergo a reversible assembly/disassembly process under external stimulus.[1−7] In the case of DNA, the assembly/disassembly of the nanoparticles can be controlled well by the temperature-related hybridization/dehybridization process of DNA.[8−12] For proteins and peptides, streptavidin−biotin[13−17] or antigen−antibody[18] interactions are usually adopted to ensure precise control over the assembly/disassembly process of the nanoparticles driven by thermodynamic binding rules.[19,20] It is well known that peptides and proteins are a kind of linear polymer composed of amino acids connected by peptide bonds, and are characterized by their amino acid sequence (primary structure)-defined secondary and three-dimensional structures and thus functions which are sensitive to a wide variety of external stimuli, including pH and temperature. Although the environment-governed balance between secondary structures (i.e., α-helix and β-sheet) of peptide building blocks had been proven to be effective in inducing the assembly/disassembly of their scaffolds,[21−23] the potential of conformation change of peptide building blocks in controlling the assembly/disassembly of inorganic nanoparticles has been poorly evaluated up till now. Poly-L-lysine (PLL) is an excellent, yet probably the simplest, model peptide which can adopt different conformations such as random coil, α-helix, or β-sheet, dependent on pH and temperature.[24,25] In this work, we demonstrated that after being functionalized by PLL, the gold nanoparticle (GNP) can undergo reversible assembly/disassembly as a result of conversion of the secondary structures of PLL on the particle surface.

Experimental Section

Materials. Poly-L-lysine (molecular weight > 8000) was procured as a hydrogen bromide salt (Peptide Institute Inc., Japan) and was used as received. The SDS-PAGE analysis showed that there were no poly-L-lysine molecules with a molecular weight higher than 10 000 in the sample. Hydrogen tetrachloroaurate trihydrate and sodium citrate tribasic dihydrate were purchased from Sigma-Aldrich. Reagent-grade NaOH and HCl were used to adjust the pH values. High-purity water with a conductivity of 18.2 MΩ cm was used in all the experiments.

Preparation and Functionalization of Gold Nanoparticles. The gold nanoparticles were prepared by reduction of $HAuCl_4$ with sodium citrate.[26] The maximum optical absorbance of the particles was at 520 nm. The polydispersity of the particles was about 4.7% as analyzed by dynamic light scattering, and the diameter was determined to be about 16 nm by TEM. The particles were concentrated by centrifugation at 8000 rpm for 30 min and redispersed in water to remove the excessive citrate. Then the stock colloidal gold sol was diluted with water to control the absorbance at about 0.8 before use. For PLL functionalization, 25 μL of PLL solution (10 mg/mL, pH = 6.5) was added rapidly into a 1.5 mL centrifuged test tube containing 500 μL of gold colloidal sol (pH = 6.5). After being shaken violently, the solution was adjusted to a different pH value by using 1 M NaOH or 1 M HCl solution.

Instrumentation. The UV−vis spectra were recorded on a Varian Cary 100 dual-beam spectrophotometer. The solutions were allowed to stand 1 min after the adjustment of the respective pH values before the UV−vis measurements. Transmission electron microscopy (TEM) images were taken using a Hitachi H-8100 IV electron microscope by using carbon-coated copper grids as substrates. The polydispersity of the

* Author to whom correspondence should be addressed. Tel: +86-431-85168170. Fax: +86-431-85168086. E-mail: wsyang@jlu.edu.cn.

[†] Key Laboratory of Surface and Interface Chemistry of Jilin Province, College of Chemistry, Jilin University.

[‡] Key Laboratory for Molecular Enzymolozy and Engineering of Ministry of Education, Jilin University.

10.1021/jp072012d CCC: $37.00
Published on Web 06/13/2007

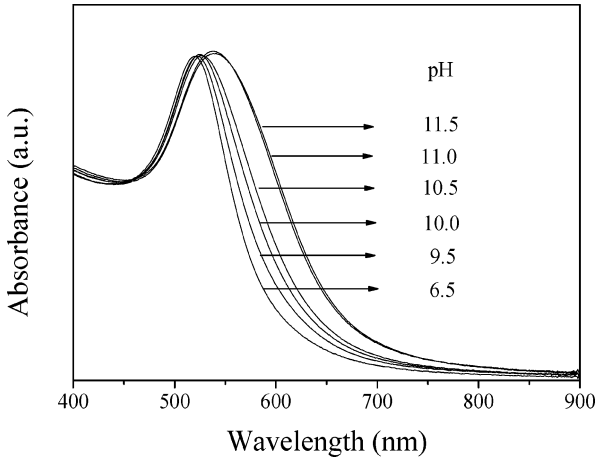

Figure 1. UV−vis spectra of a PLL-GNP solution recorded at different pH values.

particles was determined with Brookhaven ZetaPALS dynamic light scattering equipment with a BI-90Plus digital autocorrelator at a wavelength of 656 nm. Circular dichroism spectra were performed on a Jasco J-810 circular dichroism spectrophotometer using a 1 mm quartz cell. Data points for CD spectra were measured at 1 nm intervals using a bandwidth of 2 nm and response time of 4 s. After baseline correction, ellipticities in mdeg were converted to molar ellipticities by normalizing the concentration of peptide bonds. FTIR spectra were recorded with a Perkin-Elmer Spectrum One FTIR spectrometer, performed by placing the CaF_2 windows with droplets of the solution in a cabin continuously purged with dry air.[27] The citrate-stabilized gold nanoparticle was treated in the same way, and its spectrum was subtracted from that of the PLL-GNP samples. The peak-fitting procedure was applied to the spectrum to resolve its component bands according to a Lorentzian curve-fitting.[28] All the experiments were carried out at room temperature (25 °C) except these specially mentioned.

Results and Discussion

The GNP is actually stabilized through the interaction of lysine residues of PLL with the gold surface.[29] The PLL-functionalized gold nanoparticle (PLL-GNP) shows a characteristic surface plasmon resonance (SPR) band at 522 nm. Figure 1 represents a set of UV−vis spectra showing the change in the SPR band of the PLL-GNP solution in the range of pH from 6.5 to 11.5. These results clearly indicate that there is only a slight red-shift in the SPR band from 522 to 526 nm, and no obvious color change of the solution is observed with an increase of pH from 6.5 to 10.5, indicating that the PLL-GNP is well dispersed in the solution. By further increasing the pH to 11.0, the broadened, intensified, and red-shifted SPR band along with a color change of the PLL-GNP solution from red to violet suggests aggregation of the nanoparticles.[30−32] At pH 11.5, the spectrum shows only a slight change of the SPR band, meaning there is almost no further assembly of the PLL-GNP at this time.

Figure 2 shows the variation of the maximum wavelength of the SPR band with pH values. As mentioned above, the SPR band of the PLL-GNP shifts obviously from 527 to 538 nm with an increase of the pH from 10.5 to 11.0, and the color of the solution changed from red to violet which can be readily recognized by the naked eye. The SPR band of the PLL-GNP shifts gradually to a shorter wavelength with a decrease of the pH from 11.0 to 6.5, and the color of the solution changed from

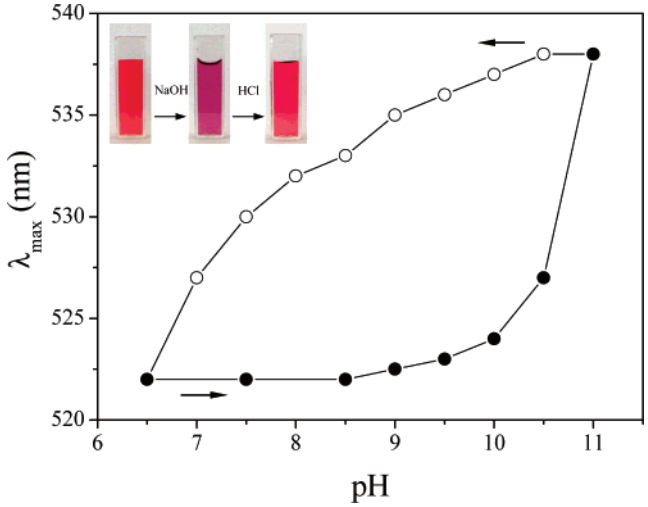

Figure 2. Variation of the maximum wavelength of the SPR band of PLL-GNP with increased (●) and decreased (○) pH values. (Inset) Color change of the PLL-GNP solution during the variation of pH values: from left to right, pH = 6.5, 11.0, and 6.5, respectively.

violet to red. This implies that the aggregated PLL-GNPs undergo disassembly upon a decrease of the pH value of the solution.

Transmission electron microscopy (TEM) observations were carried out to characterize the assembly/disassembly process of PLL-GNPs. Figure 3a shows the TEM image of PLL-GNPs at pH = 6.5, revealing the well-dispersed PLL-GNPs. At pH = 11.0, PLL-GNPs were found to undergo aggregation (Figure 3b). With a decrease of the pH value back to 6.5, the assembly of PLL-GNPs was disengaged and PLL-GNPs became well dispersed again (Figure 3c). Consistent with the UV−vis spectra, TEM observations also confirm the reversible assembly/disassembly of PLL-GNPs.

The reversibility of the pH-dependent assembly/disassembly process of the PLL-GNPs was checked by monitoring the maximum wavelength of the SPR band with cycling the pH of the solution between 6.5 and 11.0. In order to prevent accumulated ion-driven irreversible aggregation of the GNPs,[6,7] the PLL-GNP solution was dialyzed at pH 6.5 before each cycle. Figure 4 gives the variation of the maximum wavelength of the PLL-GNP solution recorded at the start and end pH values of each cycle. At the start of each cycle (pH = 6.5), the SPR band of the PLL-GNP solution presents a maximum around 522 nm. At the end of each cycle (pH = 11.0), the maximum appears around 538 nm. The pH-dependent assembly/disassembly process of the PLL-GNPs shows reasonable reversibility up to five cycles. Control experiments indicate that the gold nanoparticles without PLL on their surface did not show an obvious change of the SPR band with an increase of the pH from 6.5 to 11.5, suggesting that the pH-dependent assembly/disassembly process of the GNP is related to the PLL on its surface.

It is known that PLL shows different conformations in aqueous solution under different pH values. At neutral pH, the dominant conformation of PLL is an extended random coil due to the repulsion among the protonated lysine residues. With increased pH, the lysine residues of PLL will be deprotonated gradually and thus allow the existence of an α-helix structure and even the appearance of a β-sheet structure at appropriate temperature.[33−35] The as-prepared gold nanoparticles obtained by reduction of $HAuCl_4$ with sodium citrate did not generate CD signals in the range of wavelength investigated. The variations in CD signals of the PLL-GNP solution should be

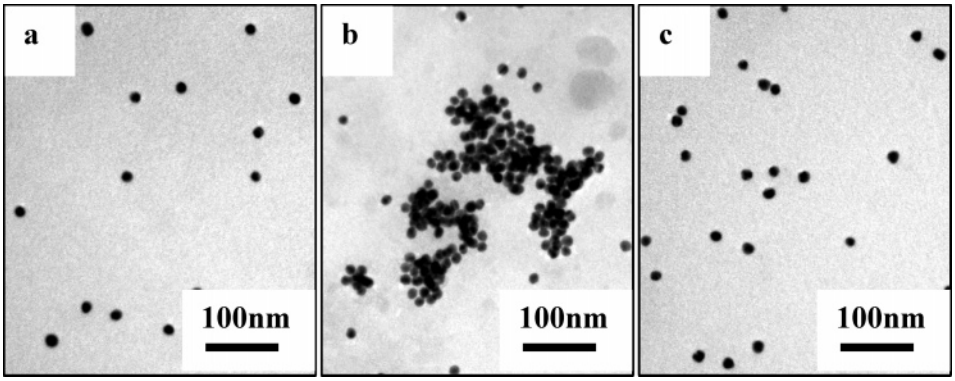

Figure 3. TEM images of PLL-GNPs observed under different pH values. (a) pH = 6.5, (b) pH = 11.0, and (c) pH = 6.5.

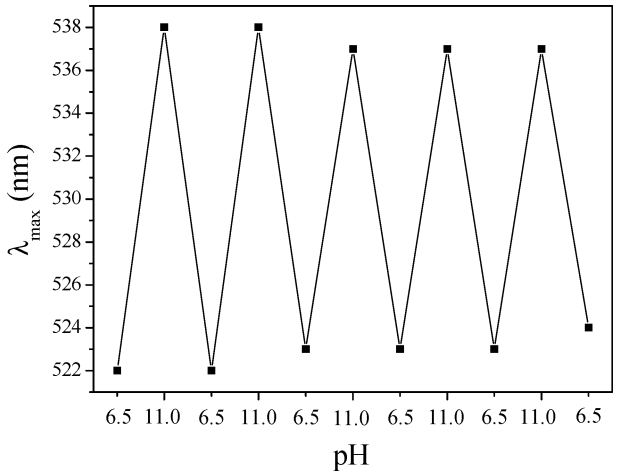

Figure 4. Maximum wavelength of the SPR band of PLL-GNP recorded at the start and end pH values of different cycles.

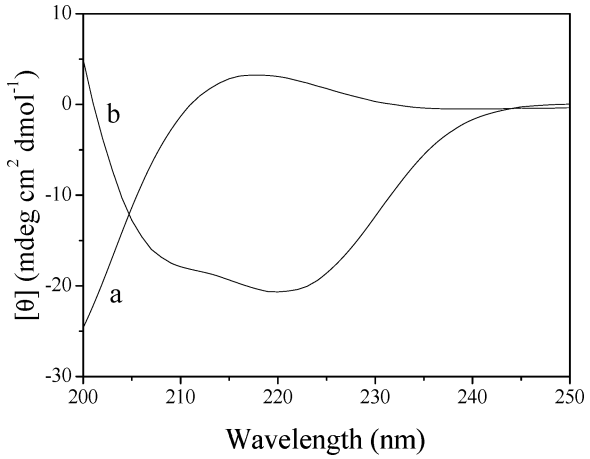

Figure 5. CD spectra of PLL-GNPs at (a) pH = 6.5 and (b) pH = 11.0.

attributed to a conformation change of PLL on the GNP surface.[36] Figure 5 presents the CD spectra of PLL-GNP solutions recorded at pH values of 6.5 and 11.0. By using Yang's reference curves,[37] the contents of secondary structures are estimated to be 62.9% random coil and 37.1% β-turn for PLL at pH 6.5 (Figure 5a). At pH 11.0, the spectrum shows double minima around 208 and 222 nm (Figure 5b), suggesting the existence of an α-helix-rich structure. Through Yang's curves, the contents are estimated to be 40.9% α-helix and 21.0% β-sheet, 30.3% random coil, and 7.8% β-turn for PLL at pH 11.0. At this pH, the lysine residues will be deprotonated almost completely since the pK_a of PLL is about 11,[38] thus allowing the existence of ordered secondary structures such as α-helix and β-sheet at the expense of less-ordered secondary structures such as random coil and β-turn.

FTIR analyses were performed to further confirm the conformational changes of PLL on the GNP surface. Figure 6a shows an IR spectrum of the PLL-GNP sample at pH 6.5 in the amide I region. After the curve-fitting, two peaks can be identified at 1650 and 1673 cm^{-1}, which are assigned to random coil and β-turn, respectively.[39] At pH 11.0, five bands are identified after the curve-fitting in the amide I region (Figure 6b). In addition to the bands of random coil at 1650cm^{-1} and β-turn at 1673 cm^{-1}, the band of α-helix at 1656 cm^{-1} and the characteristic bands of antiparallel β-sheet at 1624 and 1690 cm^{-1} are also identified.[27,28,40] PLL experiences conformation change on the GNP surface with an increase of pH from 6.5 to 11.0. At low pH, random coil and β-turn are the dominant conformation of PLL. At high pH value, α-helix and antiparallel β-sheet are formed at the expense of a part of the random coil and β-turn.

It is known that β-sheets have a greater tendency to undergo aggregation than α-helix via hydrophobic interaction.[41−43] It is proposed that the pH-dependent assembly/disassembly process of PLL-GNP is driven by the formation/collapse of the antiparallel β-sheet structure. To elucidate the effect of α-helix and β-sheets on the assembly/disassembly process of PLL-GNP, UV−vis spectra of PLL-GNP were recorded at a lower temperature, 4 °C (Figure 7). The SPR band of a PLL-GNP solution does not undergo obvious shift at different pH values, indicating there is no obvious aggregation of PLL-GNP in the range of pH investigated at this low temperature. This control experiment reveals that the pH-dependent assembly/disassembly of PLL-GNP is driven primarily by the formation of an antiparallel β-sheet structure since such low temperature will result in the absence of the β-sheet structure.[24,25] Figure 8 presents the UV−vis spectra of a PLL-GNP solution with a pH value of 11.0 recorded at different temperatures. With an increase of the temperature from 4 °C to room temperature (25 °C), the SPR band of the PLL-GNP solution undergoes an obvious red-shift and the color of the solution change from red to violet. PLL-GNP undergoes aggregation upon the formation of the antiparallel β-sheet structure. This provides us the possibility of controlling the assembly/disassembly process of PLL-GNP by changing the temperature.

On the basis of the above experimental results, the reversible assembly/disassembly process of PLL-GNP is illustrated in Figure 9.[44] At low pH, PLL on a GNP surface mainly adopts random and β-turn conformation, which is effective to stabilize the GNP. With an increase of pH, the lysine residues of PLL are deprotonated, thus allowing the existence of ordered secondary structures such as α-helix and β-sheet in addition to random coil and β-turn. If the β-sheet was excluded from a

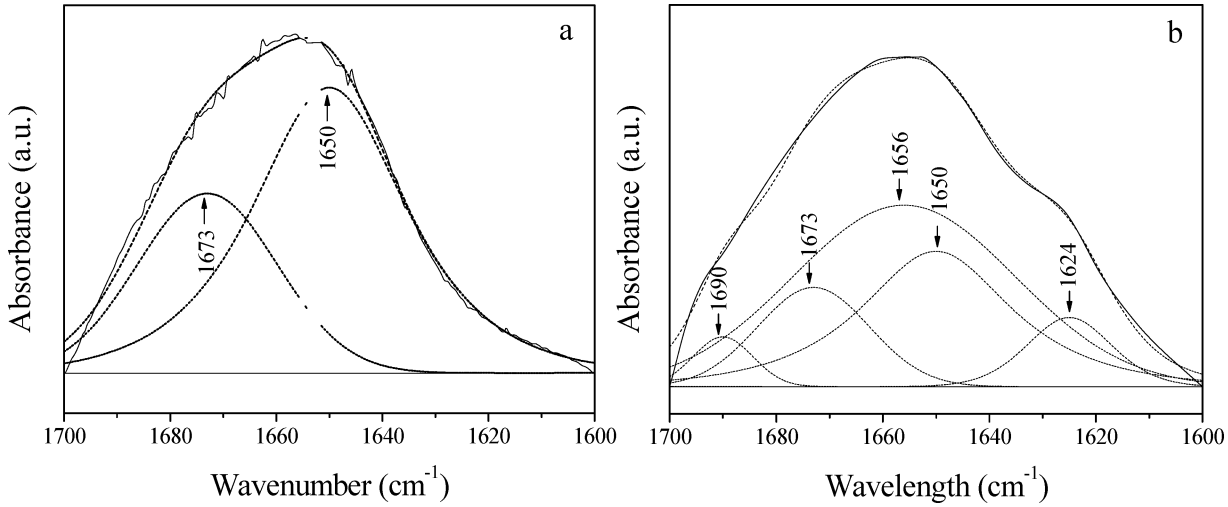

Figure 6. FTIR spectra of PLL-GNP at (a) pH = 6.5 and (b) pH = 11.0 in the amide-I region.

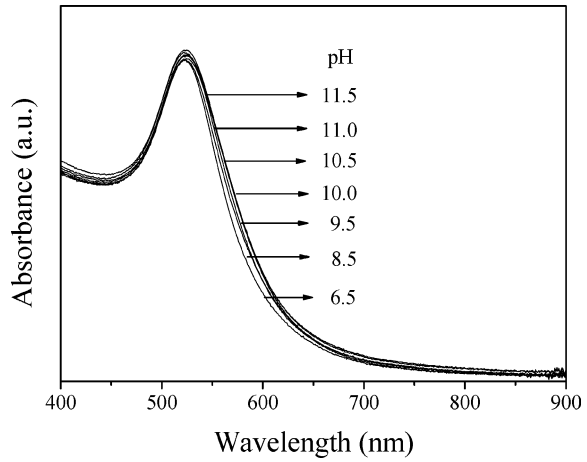

Figure 7. UV−vis spectra of PLL-GNPs under different pH values recorded at 4 °C.

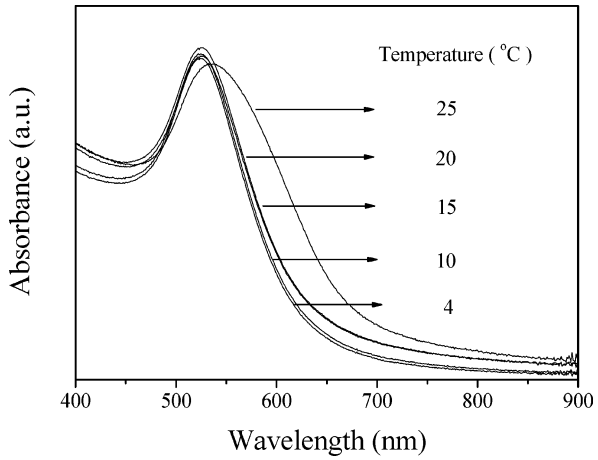

Figure 8. UV−vis spectra of PLL-GNP solution with a pH value of 11.0 recorded at different temperatures.

PLL chain, that is, by lowering the temperature to 4 °C, the aggregation of GNPs is suppressed since the remaining random coil, β-turn, and α-helix are not effective in inducing aggregation of their scaffolds.[43] One face of the β-sheet is hydrophobic in character; thus the possibility of formation of the antiparallel β-sheet structure among PLL chains from different GNPs provides the chance to induce the assembly/disassembly of GNP driven by the conformation change of PLL. It should be mentioned that the disassembly of the antiparallel β-sheet structure should be slower than its assembly process; therefore PLL-GNP solution show a hysteresis in the shift of the SPR band during the disassembly process (see Figure 2).

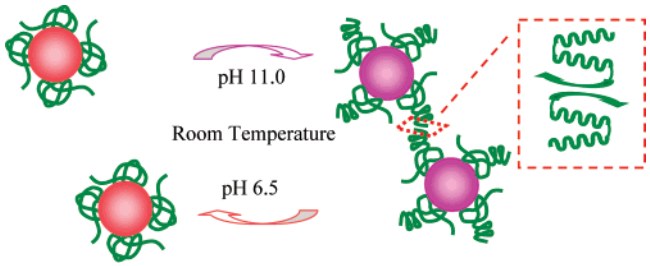

Figure 9. Schematic representation of the assembly/disassembly process of PLL-GNP induced by the conformational change of PLL. Formation of the antiparallel β-sheet structure is indicated in the dotted quadrangle region.

Conclusion

In summary, we described the reversible assembly/disassembly of PLL-GNP induced by conformational change of PLL. After the deprotonization of lysine residues of PLL at high pH, GNPs undergo aggregation due to the appearance of α-helix and β-sheet at the expense of a part of random coil and β-turn structures. Upon the protonization of the lysine residues of PLL by decreasing the pH, GNPs become well dispersed again due to the disappearance of α-helix and β-sheet in PLL. The formation/collapse of antiparallel β-sheet structure among PLL chains from adjacent GNPs is of primary importance in inducing the assembly/disassembly of PLL-GNPs. Such a study on the conformational change induced reversible assembly/disassembly process means that the GNP is a potential probe for following the conformational change of peptides and proteins.

Acknowledgment. This work was supported by the National Natural Science Foundation of China, the Key Project, and the Program for NCET in the University of Chinese Ministry of Education.

References and Notes

(1) Niemeyer, C. M. *Angew. Chem., Int. Ed.* **2001**, *40*, 4128.
(2) Jiang, L.; Zhang, H.; Zhuang, J.; Yang, B.; Yang, W.; Li, T.; Sun, C. *Adv. Mater.* **2005**, *17*, 2066.
(3) Katz, E.; Willner, I. *Angew. Chem., Int. Ed.* **2004**, *43*, 6042.
(4) Srivastava, S.; Verma, A.; Frankamp, B. L.; Rotello, V. M. *Adv. Mater.* **2005**, *17*, 617.

(5) Basu, S.; Panigrahi, S.; Praharaj, S.; Ghosh, S. K.; Pande, S.; Jana, S.; Pal, T. *New J. Chem.* **2006**, *30*, 1333.
(6) Jung, Y. H.; Lee, K.-B.; Kim, Y.-G.; Choi, I. S. *Angew. Chem., Int. Ed.* **2006**, *45*, 5960.
(7) Si, S.; Mandal, T. K. *Langmuir* **2007**, *23*, 190.
(8) Mirkin, C. A.; Letsinger, R. L.; Mucic, R. C.; Storhoff, J. J. *Nature* **1996**, *382*, 607.
(9) Alivisatos, A. P.; Johnsson, K. P.; Peng, X.; Wilson, T. E.; Loweth, C. J.; Bruchez, M. P.; Schultz, P. G. *Nature* **1996**, *382*, 609.
(10) Mirkin, C. A. *Inorg. Chem.* **2000**, *39*, 2258.
(11) Pellegrino, T.; Kudera, S.; Liedl, T.; Javier, A. M.; Manna, L.; Parak, W. J. *Small* **2005**, *1*, 48.
(12) Sadasivan, S.; Dujardin, E.; Li, M.; Johnson, C. J.; Mann, S. *Small* **2005**, *1*, 103.
(13) Niemeyer, C. M.; Burger, W.; Peplies, J. *Angew. Chem., Int. Ed.* **1998**, *37*, 2265.
(14) Connolly, S.; Fitzmaurice, D. *Adv. Mater.* **1999**, *11*, 1202.
(15) Aslan, K.; Luhrs, C. C.; Perez-Luna, V. H. *J. Phys. Chem. B* **2004**, *108*, 15631.
(16) Gole, A.; Murphy, C. J. *Langmuir* **2005**, *21*, 10756.
(17) Crespo-Biel, O.; Ravoo, B. J.; Reinhoudta, D. N.; Huskens, J. *J. Mater. Chem.* **2006**, *16*, 3997.
(18) Shenton, W.; Davies, S. A.; Mann, S. *Adv. Mater.* **1999**, *11*, 449.
(19) Larsericsdotter, H.; Oscarsson, S.; Buijs, J. *J. Colloid Interface Sci.* **2001**, *237*, 98.
(20) Brockhaus, M.; Ganz, P.; Huber, W.; Bohrmann, B.; Loetscher, H. R.; Seelig, J. *J. Phys. Chem. B* **2007**, *111*, 1238.
(21) Maxim, M. G.; Ceyhan, B.; Niemeyer, C. M.; Woolfson, D. N. *J. Am. Chem. Soc.* **2003**, *125*, 9388.
(22) Zhang, S. *Nat. Biotechnol.* **2003**, *21*, 1171.
(23) Stevens, M. M.; Flynn, N. T.; Wang, C.; Tirrell, D. A.; Langer, R. *Adv. Mater.* **2004**, *16*, 915.
(24) Davidson, B.; Fasman, G. D. *Biochemistry* **1967**, *6*, 1616.
(25) Greenfieldi, N.; Fasman, G. D. *Biochemistry* **1969**, *8*, 4108.
(26) Grabar, K. C.; Freeman, R. G.; Hornmer, M. B.; Natan, M. J. *Anal. Chem.* **1995**, *67*, 735.
(27) Wolkers, W. F.; Kilsdonk, M. G.; Hoekstra, F. A. *BBA-Gen. Subjects* **1998**, *1425*, 127.
(28) May, L. M.; Russell, D. A. *Analyst* **2002**, *127*, 1589.
(29) Xu, L.; Guo, Y.; Xie, R.; Zhuang, J.; Yang, W.; Li, T. *Nanotechnology* **2002**, *13*, 725.
(30) Lazarides, A. A.; Schatz, G. C. *J. Phys. Chem. B* **2000**, *104*, 460.
(31) Storhoff, J. J.; Lazarides, A. A.; Mucic, R. C.; Mirkin, C. A.; Letsinger, R. L.; Schatz, G. C. *J. Am. Chem. Soc.* **2000**, *122*, 4640.
(32) Zhong, Z.; Patskovskyy, S.; Bouvrette, P.; Luong, J. H. T.; Gedanken, A. *J. Phys. Chem. B* **2004**, *108*, 4046.
(33) Smirnovas, V.; Winter, R.; Funck, T.; Dzwolak, W. *J. Phys. Chem. B* **2005**, *109*, 19043.
(34) Dzwolak, W.; Muraki, T.; Kato, M.; Taniguchi, Y. *Biopolymers* **2004**, *73*, 463.
(35) General, S.; Thunemann, A. F. *Int. J. Pharm.* **2001**, *230*, 11.
(36) Li, T.; Park, H. G.; Lee, H.-S.; Choi, S.-H. *Nanotechnology* **2004**, *15*, S660.
(37) Chapman, R. N.; Dimartino, G.; Arora, P. S. *J. Am. Chem. Soc.* **2004**, *126*, 12252.
(38) Murthy, V. S.; Cha, J. N.; Stucky, G. D.; Wong, M. S. *J. Am. Chem. Soc.* **2004**, *126*, 5292.
(39) Dong, A.; Huang, P.; Caughey, W. S. *Biochemistry* **1990**, *29*, 3303.
(40) Surewicz, W. K.; Mantsch, H. H.; Chapman, D. *Biochemistry* **1993**, *32*, 389.
(41) Garrett, R. H.; Grisham, C. M. *Biochemistry*, 2nd ed.; Harcourt, Inc.: Orlando, FL, 1999; Chapter 6.
(42) Rozenberg, M.; Shoham, G. *Biophys. Chem.* **2007**, *125*, 166.
(43) Jarvet, J.; Damberg, P.; Bodell, K.; Goran Eriksson, L. E.; Graslund, A. *J. Am. Chem. Soc.* **2000**, *122*, 4261.
(44) It is noted that the particles were not purified after the poly-L-lysine modification and there should be free poly-L-lysine in the solution. We also carried out the same experiments after purifying the particles by centrifugation or dialysis. The pH- or temperature-dependent aggregation behavior of the particles was almost the same before and after the purification. The main difference came from the CD spectrum, the signals became too weak to identify the conformation change of the poly-L-lysine. Therefore, the free poly-L-lysine molecules were not included in the proposed scheme since they were not necessary for the aggregation process.